International Journal of Automotive Technology, Vol. 6, No. 5, pp. 491–499 (2005)

1229-9138/2005/023-08

CRASHWORTHINESS IMPROVEMENT OF VEHICLE-TO-RIGID FIXED BARRIER IN FULL FRONTAL IMPACT USING NOVEL VEHICLE'S FRONT-END STRUCTURES

A. M. ELMARAKBI* and J. W. ZU

Department of Mechanical and Industrial Engineering, University of Toronto, Toronto, Ontario, M5S 3G8, Canada

(Received 10 November 2004; Revised 16 May 2005)

ABSTRACT–There are different types of vehicle impacts recorded every year, resulting in many injuries and fatalities. The severity of these impacts depends on the aggressivety and incompatibility of vehicle-to-roadside hardware impacts. The aim of this paper is to investigate and to enhance crashworthiness in the case of full barrier impact using a new idea of crash improvement. Two different types of smart structures have been proposed to support the function of the existing vehicle. The work carried out in this paper includes developing and analyzing mathematical models of vehicle-to-barrier impact for the two types of smart structures. It is proven from analytical analysis that the mathematical models can be used in an effective way to give a quick insight of real life crashes. Moreover, it is shown that these models are valid and flexible, and can be useful in optimization studies.

KEY WORDS : Crashworthiness, Full frontal impact, Smart front-end structure, Analytical anlysis

1. INTRODUCTION

Crashworthiness improvement and vehicle frontal impact mitigation have become one of the major research areas in automotive engineering. The increasing public awareness of safety issues and the increasing legislative requirements have increased the pressure on vehicle manufacturers to improve the vehicle crashworthiness.

There are two types of smart structures proposed to improve the vehicle crashworthiness. The first type consists of two extendable controlled hydraulic cylinders integrated with the front-end longitudinal members as shown in Figure 1. The second type consists of two non-extendable (fixed) hydraulic cylinders parallel to the longitudinal members as shown in Figure 2.

Frontal crashworthiness improvement using hydraulic cylinders was initially developed by Schwarz in (1971). In his research, hydraulic energy absorption systems were designed to mitigate high speed impacts up to 80 km/h. Moreover, using hydraulic cylinders to absorb crash energy at high speed collisions were investigated by Appel *et al.* (1973) to improve the crashworthiness of motor vehicles. The basic idea was tested by Rupp (1974). In his research, he utilized hydraulic buffers to maximize the absorbed impact energy. He used two extendable, independently controlled hydraulic buffers integrated with the front-end longitudinal members. Rupp's study aimed to mitigate high-speed frontal impacts. Five different strokes were used and different impact speeds were investigated ranging from 36 km/h to 73 km/h. Recently, Jawad *et al.* (1999, 2001) used hydraulic cylinders to mitigate high

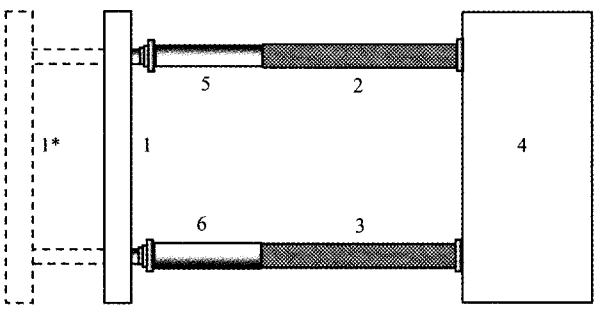

1 Bumper
1* Bumper in the extendable position
2 Right longitudinal member
3 Left longitudinal member
4 Body of the vehicle including the occupant
5 Right hydraulic cylinder
6 Left hydraulic cylinder

Figure 1. Extendable smart structure.

*Corresponding author. e-mail: ahmed.elmarakbi@utoronto.ca

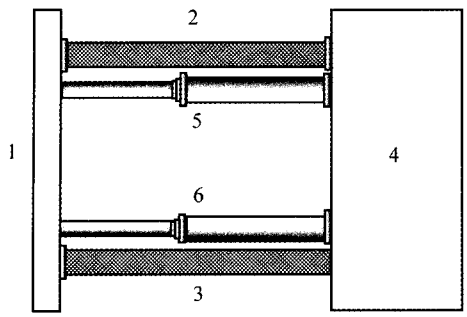

Figure 2. Fixed smart structure.

speed frontal impact. In their works, two controlled hydraulic cylinders were proposed to be extended prior to collision and absorb impact energy upon engagement with other body using radar collision prediction sensors. High speed collisions at 36 km/h, 56 km/h, and 64 km/h were investigated. Furthermore, Witteman *et al.* (1998, 2001) used non extendable hydraulic cylinders improve the frontal impact at initial crash speed of 56 km/h. In addition, Witteman (1999) presented a study showing that increased protection for the entire collision spectrum can be obtained by a frontal structure consisting of two special longitudinal members. The longitudinal members are supported by a cable connection system for symmetric force distribution. Similar research by Clark (1994) presented another solution to improve vehicle frontal crashworthiness and to reduce the crash severity. In his work, he developed an extended airbag bumper system. With radar detection a collision is predicted and a large airbag deploys in front of the bumper.

In automotive industry, development of smart structures is continuously evolved by safety engineers. There are a few patents on smart structures since 1976 by Ellis (1976), Reuber *et al.* (1994), and Wang (1994), which concentrate on the design procedures. However, there is a lack of research with regard to the analysis of smart structures.

The analysis of smart structures is powerful for redesign of systems to improve their performance. Furthermore, the analysis of smart structures facilitates the commercialization stage of the design. This paper seeks to develop mathematical models of the smart structures in full frontal barrier impact and to find analytical solutions to these models for crashworthiness study. A review of the previous work shows that little has been done for the development of simplified models for automotive crash problems in general, and smart structures in particular.

The development of such models is desirable for use in the initial concept design stage of automotive structures before costly and time consuming large-scale finite element analysis is performed.

2. MATHEMATICAL MODELS

Mass-spring models are often applied in car research and development for car-to-car crashes, either in a simple form with a few masses or somewhat more complex form with about 50 masses (Coo *et al.*, 1991). Lumped mass models have been used since the early 70's for the analysis and design of automotive structures for safety during crash (Kamal, 1970).

The mathematical models shown in Figures 3 and 4 represent the two types of smart structures in the case of full barrier frontal impact. The vehicle impacts the rigid barrier with an initial velocity v_0. The stiffness element shown as a spring with stiffness k is the plastic deformation part representing the front-end structure. The hydraulic cylinders are represented by a damper with damping coefficient c.

A representation of the occupant inside the vehicle body is also shown in Figures 3 and 4. The occupant-restraint characteristics of the seat belt and the airbag are represented by stiffness k_o and damping coefficient c_o. The masses of the vehicle body and the occupant are represented by m and m_o, respectively.

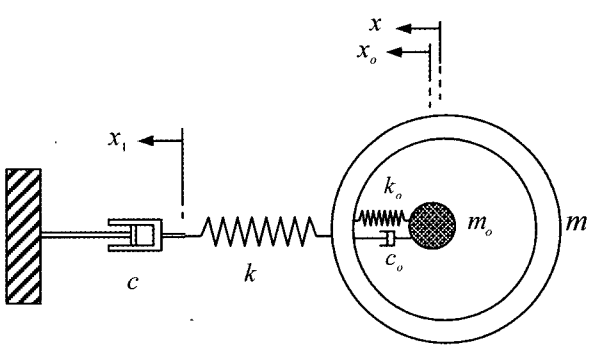

Figure 3. Mathematical model of extendable smart vehicle- to -Rigid Barrier full frontal collision.

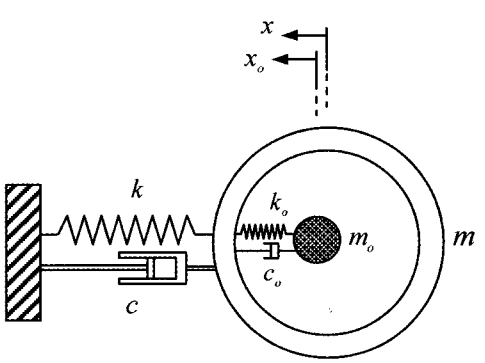

Figure 4. Mathematical model of fixed smart vehicle - to-Rigid Barrier full frontal collision.

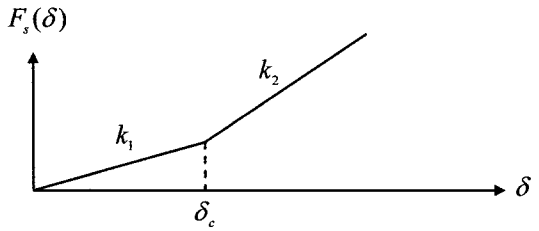

Figure 5. Force-deformation characteristic of the vehicle.

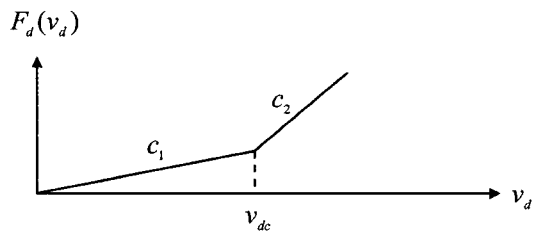

Figure 6. Force-velocity characteristic of the hydraulic cylinder.

In case of crash analysis, the mass is always constant while the damping and stiffness are not; they mainly depend on the velocity and displacement values. In this paper, the forces of the plastic spring $F_s(\delta)$ and the damper $F_d(v_d)$ are defined as follows:

1. The force generated by the plastic spring of the vehicle shown in Figure 5 can be written as

$$F_s(\delta) = k \cdot \delta - F_c \tag{1a}$$

where $k = k_1$ $F_c = 0$ $\delta \le \delta_c$ (1b)

$k = k_2$ $F_c = (k_2 - k_2) \cdot \delta_c$ $\delta > \delta_c$ (1c)

2. The damping force generated by the hydraulic cylinder shown in Figure 6 is given by

$$F_d(v_d) = c \cdot v_d - F_c^* \tag{2a}$$

where $c = c_1$ $F_c^* = 0$ $v_d \le v_{dc}$ (2b)

$c = c_2$ $F_c^* = (c_2 - c_1) \cdot v_{dc}$ $v_d > v_{dc}$ (2c)

3. The force generated by the spring on the occupant shown in Figure 7 is written in the following

$$F_{so}(\delta_o) = k \cdot (\delta_o - \delta_{co}) \tag{3a}$$

where $k = 0$ $\delta_o \le \delta_{co}$ (3b)

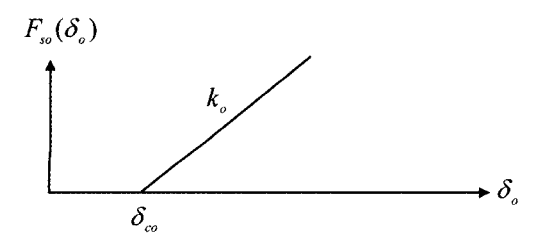

Figure 7. Force-deformation characteristic of the occupant.

$k = k_o$ $\delta_o > \delta_{co}$ (3c)

The damping coefficient of the occupant is taken as 50% of the critical damping (Cacciaube, 1972).

$$c_o = \sqrt{k_o m_o} \tag{4a}$$

and the damping force on the occupant is given by

$$F_{do}(v_o) = c \cdot (v_o - v_{co}) \tag{4b}$$

where $c = 0$ $v_o \le v_{co}$ (4c)

$c = c_o$ $v_o > v_{co}$ (4d)

where δ_{co} is the initial slack length. The slack length represents the relative displacement of the occupant δ_o before the seatbelt becomes effective. In addition, the relative velocity of the occupant when the seatbelt becomes effective is defined by v_{co}

The deformation of the plastic spring and the velocity of the hydraulic cylinder are respectively defined as follows:

Case I: Extendable smart structure-to-barrier impact

$$\delta = x - x_1, \qquad v_d = \dot{x}_1 \tag{5}$$

Case II: Fixed smart structure-to-barrier impact

$$\delta = x, \qquad v_d = \dot{x} \tag{6}$$

The deformation of the spring and the velocity of the damper of the occupant are respectively defined as

$$\delta_o = x_o - x, \qquad v_o = \dot{x}_o - \dot{x} \tag{7}$$

3. CLOSED FORM SOLUTIONS

3.1. Exendable Smart Stuctures

The initial impact event when a vehicle hits an obstacle (barrier, vehicle, etc.) is referred to as the first or primary impact. The following event when the occupant moves within the vehicle and impacts the interior is called the secondary impact.

3.1.1. Primary impact

The equations of motion for the system shown in Figure 3 can be written as follows:

$$m\ddot{x} + F_s(\delta) = 0 \tag{8}$$

$$F_d(v_d) - F_s(\delta) = 0 \tag{9}$$

Substituting Equations (1), (2) and (5) into Equations (8) and (9) yields

$$\ddot{x} + \frac{k}{m}(x - x_1) = \frac{F_c}{m} \tag{10}$$

$$\dot{x} - \frac{k}{c}(x - x_1) = -\frac{F_c - F_c^*}{c} \tag{11}$$

The following parameters are introduced

$$\alpha = \frac{k}{c} = \frac{k}{\xi_1 c_{c1}}, \ \beta = \frac{k}{m} = \omega^2, f_1 = \frac{F_c - F_c^*}{c}, f_2 = \frac{F_c}{m} \tag{12}$$

where the damping ratio is $x_1 = c/c_{c1}$, c_{c1} is the critical damping, and ω is the natural frequency. Now, choose state variables y_i and initial conditions as

$$x_1 = y_1, \quad \dot{x}_1 = \dot{y}_1, \quad x = y_2, \quad \dot{x} = \dot{y}_2 = y_3, \quad \ddot{x} = \dot{y}_3 \tag{13}$$

$$y_1(0) = (x_1)_0, \quad y_2(0) = x_0, \quad y_3(0) = v_0 \tag{14}$$

Equations (10) and (11) are rewritten as

$$\begin{bmatrix} \dot{y}_1 \\ \dot{y}_2 \\ \dot{y}_3 \end{bmatrix} = \begin{bmatrix} -\alpha & \alpha & 0 \\ 0 & 0 & 1 \\ \beta & -\beta & 0 \end{bmatrix} \begin{bmatrix} y_1 \\ y_2 \\ y_3 \end{bmatrix} + \begin{bmatrix} -f_1 \\ 0 \\ f_2 \end{bmatrix} \tag{15}$$

where $A = \begin{bmatrix} -\alpha & \alpha & 0 \\ 0 & 0 & 1 \\ \beta & -\beta & 0 \end{bmatrix}$ $u(\tau) = \begin{bmatrix} -f_1 \\ 0 \\ f_2 \end{bmatrix}$

$$(y_i)_0 = \begin{bmatrix} (x_1)_0 \\ x_0 \\ v_0 \end{bmatrix} \tag{16}$$

By introducing the coordinate transformation,

$$y_i = Pz_i \tag{17}$$

The solution of Equation (15) can be obtained using modal analysis as follows:

$$z_i = e^{\Lambda t}(z_i)_0 + e^{\Lambda t}\int_0^t e^{-\Lambda \tau} U(\tau) d\tau \tag{18}$$

where P and Λ are the modal matrix and the diagonal matrix of the eigenvalues, respectively.

$$P = \begin{bmatrix} 1 & \frac{-\alpha}{\beta} & \frac{-\alpha}{\beta} \\ 1 & \frac{\alpha + \sqrt{\alpha^2 - 4\beta}}{2\beta} & \frac{\alpha - \sqrt{\alpha^2 - 4\beta}}{2\beta} \\ 0 & 1 & 1 \end{bmatrix} \tag{19}$$

$$\Lambda = \begin{bmatrix} 0 & 0 & 0 \\ 0 & \frac{-\alpha + \sqrt{\alpha^2 - 4\beta}}{2} & 0 \\ 0 & 0 & \frac{-\alpha - \sqrt{\alpha^2 - 4\beta}}{2} \end{bmatrix} \tag{20}$$

Moreover, $U(\tau)$ and $(z_i)_0$ are determined by the following equations:

$$U(\tau) = P^{-1}u(\tau) = \begin{bmatrix} -f_1 + \frac{\alpha f_2}{\beta} \\ \frac{-f_1\beta + (\lambda_2 + \alpha)f_2}{\lambda_2 - \lambda_3} \\ \frac{f_1\beta - (\lambda_2 + \alpha)f_2}{\lambda_2 - \lambda_3} \end{bmatrix} \tag{21}$$

$$(z_i)_0 = P^{-1}(y_i)_0 = \begin{bmatrix} (x_1)_0 + \frac{\alpha v_0}{\beta} \\ \frac{\beta((x_1)_0 - x_0) + (\lambda_2 + \alpha)v_0}{\lambda_2 - \lambda_3} \\ \frac{-\beta((x_1)_0 - x_0) - (\lambda_3 + \alpha)v_0}{\lambda_2 - \lambda_3} \end{bmatrix} \tag{22}$$

By substituting Equations (19–22) into Equation (18), a general solution of z_i can be obtained as:

$$z_i = \begin{bmatrix} (x_1)_0 + \frac{\alpha v_0}{\beta} - f_1 t + \frac{\alpha f_2 t}{\beta} \\ \frac{e^{\lambda_2 t}(\beta((x_1)_0 - x_0) + (\lambda_2 + \alpha)v_0)}{\lambda_2 - \lambda_3} + \frac{(\beta f_1 - f_2(\lambda_2 + \alpha))(1 - e^{\lambda_2 t})}{\lambda_2(\lambda_2 - \lambda_3)} \\ \frac{-e^{\lambda_3 t}(\beta((x_1)_0 - x_0) - (\lambda_3 + \alpha)v_0)}{\lambda_2 - \lambda_3} + \frac{(\beta f_1 - f_2(\lambda_3 + \alpha))(1 - e^{\lambda_3 t})}{\lambda_3(\lambda_2 - \lambda_3)} \end{bmatrix} \tag{23}$$

The closed form solution of x_i can be obtained by substituting Equations (13), (19), and (23) into Equation (17) as

$$x_1 = (x_1)_0 + \frac{\alpha v_0}{\beta} + Bt - \frac{\alpha}{\beta(\lambda_2 - \lambda_3)} * \Big[e^{\lambda_2 t}(\beta((x_1)_0 - x_0) + (\lambda_2 + \alpha)v_0) - e^{\lambda_3 t}(\beta((x_1)_0 - x_0) + (\lambda_3 + \alpha)v_0) + \frac{(1 - e^{\lambda_2 t})C}{\lambda_2} - \frac{(1 - e^{\lambda_3 t})D}{\lambda_3} \Big] \tag{24}$$

$$x = (x_1)_0 + \frac{\alpha v_0}{\beta} + Bt + \frac{\lambda_3}{\beta(\lambda_2 - \lambda_3)} * \Big[e^{\lambda_2 t}(\beta((x_1)_0 - x_0) + (\lambda_2 + \alpha)v_0) + \frac{(1 - e^{\lambda_2 t})C}{\lambda_2} \Big] - \frac{\lambda_2}{\beta(\lambda_2 - \lambda_3)} * \Big[e^{\lambda_3 t}(\beta((x_1)_0 - x_0)) + ((\lambda_3 + \alpha)v_0) + \frac{(1 - e^{\lambda_3 t})D}{\lambda_3} \Big] \tag{25}$$

The velocity and the deceleration of the passenger compartment can be obtained by differentiation of Equation (25) as

$$\dot{x} = B + \frac{\lambda_2\lambda_3}{\beta(\lambda_2 - \lambda_3)} \Big[e^{\lambda_2 t}(\beta((x_1)_0 - x_0) + (\lambda_2 + \alpha)v_0) - e^{\lambda_3 t}(\beta((x_1)_0 - x_0) + (\lambda_3 + \alpha)v_0) - \frac{e^{\lambda_2 t}C}{\lambda_2} + \frac{e^{\lambda_3 t}D}{\lambda_3} \Big] \tag{26}$$

$$\ddot{x} = \frac{\lambda_2\lambda_3}{\beta(\lambda_2 - \lambda_3)} [\lambda_2 e^{\lambda_2 t}(\beta((x_1)_0 - x_0) + (\lambda_2 + \alpha)v_0) - \lambda_3 e^{\lambda_3 t}(\beta((x_1)_0 - x_0) + (\lambda_3 + \alpha)v_0) - e^{\lambda_2 t}C + e^{\lambda_3 t}D] \tag{27}$$

Where $\lambda_1 = 0$, $\lambda_2 = \frac{-\alpha + \sqrt{\alpha^2 - 4\beta}}{2}$,

$\lambda_3 = \frac{-\alpha - \sqrt{\alpha^2 - 4\beta}}{2}$ $B = -f_1 + \frac{\alpha f_2}{\beta}$,

$$C = \beta f_1 - f_2(\lambda_2 + \alpha), \qquad D = \beta f_1 - f_2(\lambda_3 + \alpha) \quad (28)$$

From the eigenvlues in Equation (28), the critical damping c_{c1} can be obtained if $\alpha^2 - 4\beta$ is zero as follows:

$$c_{c1} = \frac{\omega m}{2} \quad (29)$$

Substituting Equation (29) into (12) yields

$$\alpha = \frac{2\omega}{\xi_1} \quad (30)$$

It is worthwhile noting that if $(\alpha^2 - 4\beta) < 0$, the values of λ_2 and λ_3 from Equation (28) become imaginary and are given by

$$\lambda_2 = \frac{-\omega + \omega_d i}{\xi_1}, \quad \lambda_3 = \frac{-\omega - \omega_d i}{\xi_1} \quad (31)$$

where ω_{d1} is damped natural frequency and can be defined as

$$\omega_{d1} = \sqrt{\xi_1^2 - 1} \quad (32)$$

The general solution in this case can be written as follows:

$$x_1 = (x_1)_0 + \frac{2(v_0 + f_1)}{\xi_1\omega} - \frac{4f_2}{\xi_1^2\omega^2} - f_1 t + \frac{2f_2 t}{\xi_1\omega} - \frac{2}{\xi_1\omega}\left[\left(v_0 + f_1 - \frac{2f_2}{\xi_1\omega}\right)\cdot e^{\frac{-\omega}{\xi_1}t}\cos\left(\frac{\omega_{d1}}{\xi_1}t\right) - 2\left(\frac{\omega((x_1)_0 - (x)_0)}{\omega_{d1}} + \frac{v_0 + f_1}{\xi_1\omega_{d1}} - \frac{f_2}{\xi_1^2\omega\omega_{d1}} + \frac{\omega_d f_2}{\xi_1^2\omega^3}\right)\cdot e^{\frac{-\omega}{\xi_1}t}\sin\left(\frac{\omega_{d1}}{\xi_1}t\right)\right] \quad (33)$$

$$x = A_1 + Bt + C_1 e^{\frac{-\omega}{\xi_1}t}\cos\left(\frac{\omega_{d1}}{\xi_1}t\right) + D_1 e^{\frac{-\omega}{\xi_1}t}\sin\left(\frac{\omega_{d1}}{\xi_1}t\right) \quad (34)$$

The velocity and the deceleration of the passenger compartment can be obtained by differentiation of Equation (34) as

$$\dot{x} = B - \left(C_1\frac{\omega_{d1}}{\xi_1} + D_1\frac{\omega}{\xi_1}\right)e^{\frac{-\omega}{\xi_1}t}\sin\left(\frac{\omega_{d1}}{\xi_1}t\right) - \left(C_1\frac{\omega}{\xi_1} - D_1\frac{\omega_{d1}}{\xi_1}\right)e^{\frac{-\omega}{\xi_1}t}\cos\left(\frac{\omega_{d1}}{\xi_1}t\right) \quad (35)$$

$$\ddot{x} = \left(D_1\left(\frac{\omega}{\xi_1}\right)^2 - D_1\left(\frac{\omega_{d1}}{\xi_1}\right)^2 + 2C_1\frac{\omega\omega_{d1}}{\xi_1^2}\right)\cdot e^{\frac{-\omega}{\xi_1}t}\sin\left(\frac{\omega_{d1}}{\xi_1}t\right) + \left(C_1\left(\frac{\omega}{\xi_1}\right)^2 - C_1\left(\frac{\omega_{d1}}{\xi_1}\right)^2 + 2D_1\frac{\omega\omega_{d1}}{\xi_1^2}\right)\cdot e^{\frac{-\omega}{\xi_1}t}\cos\left(\frac{\omega_{d1}}{\xi_1}t\right) \quad (36)$$

where $A_1 = (x_1)_0 + \frac{2(v_0 + f_1)}{\xi_1\omega} + \frac{f_2}{\omega^2} - \frac{4f_2}{\xi_1^2\omega^2}$,

$$B = -f_1 + \frac{\alpha f_2}{\beta},$$

$$C_1 = \left((x)_0 - (x_1)_0 + \frac{4f_2}{\xi_1^2\omega^2} - \frac{2(v_0 + f_1)}{\xi_1\omega} - \frac{f_2}{\omega^2}\right),$$

$$D_1 = \left(\frac{\xi_1 f_1}{\omega_{d1}} - \frac{2f_1}{\xi_1\omega_{d1}} - \frac{2f_2}{\omega\omega_{d1}} + \frac{4f_2}{\xi_1^2\omega\omega_{d1}} - \frac{\omega((x_1)_0 - (x)_0)}{\omega_{d1}} + \frac{\xi_1 v_0}{\omega_{d1}} - \frac{2v_0}{\xi_1\omega_{d1}}\right) \quad (37)$$

3.1.2. Secondary impact

The equations of motion of the occupant can be written as follows:

$$m_o\ddot{x}_o + F_{so}(\delta_o) + F_{do}(v_o) = 0 \quad (38)$$

Substituting Equations (3), (4), and (7) into Equation (38) yields

$$m_o\ddot{x}_o + c_o\dot{x}_o + k_o x_o = f(t) \quad (39)$$

where $f(t) = c_o(\dot{x} + v_{co}) + k_o(x + \delta_{co})$ (40)

The general solution of Equation (39) can be determined in the following form

$$x_o(t) = e^{-\xi_o\omega_o t}(a\sin\omega_{do}t + b\cos\omega_{do}t) + \frac{1}{m_o\omega_{do}}\int_o^t f(\tau)e^{-\xi_o\omega_o(t-\tau)}\sin\omega_{do}(t-\tau)d\tau \quad (41)$$

The occupant is subjected to the following initial conditions

$$x_o(0) = 0, \qquad \dot{x}_o(0) = v_o \quad (42)$$

Using the initial conditions of the occupant, Equation (41) can be rewritten as

$$x_o(t) = e^{-\xi_o\omega_o t}\left(\frac{v_o}{\omega_{do}}\sin(\omega_{do}t)\right) + \frac{\sin(\omega_{do}t)e^{-\xi_o\omega_o t}}{m_o\omega_{do}}\int_o^t f(\tau)e^{\xi_o\omega_o\tau}\cos(\omega_{do}\tau)d\tau - \frac{\cos(\omega_{do}t)e^{-\xi_o\omega_o t}}{m_o\omega_{do}}\int_o^t f(\tau)e^{\xi_o\omega_o\tau}\sin(\omega_{do}\tau)d\tau \quad (43)$$

where

$$\xi_o = \frac{c_o}{c_{co}}, \qquad c_{co} = 2m_o\omega_o, \qquad \omega_{do} = \sqrt{1 - \xi_o^2} \quad (44)$$

The velocity and the deceleration of the occupant can be obtained by differentiation of Equation (43).

3.2. Fixed Smart Structure

3.2.1. Primary impact

The equations of motion for the system shown in Figure 4 can be written as follows:

$$m\ddot{x} + F_s(\delta) + F_d(v_d) = 0 \quad (44)$$

Substituting Equations (1), (2), and (6) into Equation (44) yields

$$m\ddot{x} + c\,\dot{x} + k\,x = F_c^* + F_c \tag{45}$$

The following parameters are introduced

$$\psi = \frac{c}{m} = \frac{\xi c_c}{m}, \quad \beta = \frac{k}{m} = \omega^2, \quad f_1 = \frac{F_c^* + F_c}{m} \tag{46}$$

Equation (45) is rewritten as

$$\ddot{x} + \psi \cdot \dot{x} + \beta \cdot x = f_1 \tag{47}$$

Now, choose state variables y_i and initial conditions as follows:

$$x = y_1, \qquad \dot{x} = y_2 = \dot{y}_1, \qquad \ddot{x} = \dot{y}_2 \tag{48}$$

$$y_1(0) = x_0, \qquad y_2(0) = v_0 \tag{49}$$

and rewrite the equation of motion in term of y_i as follows:

$$\begin{bmatrix} \dot{y}_1 \\ \dot{y}_2 \end{bmatrix} = \begin{bmatrix} 0 & 1 \\ -\beta & -\psi \end{bmatrix} \begin{bmatrix} y_1 \\ y_2 \end{bmatrix} + \begin{bmatrix} 0 \\ f_1 \end{bmatrix} \tag{50}$$

Using the same procedure as before, the general solution of Equation (50) can be obtained in the following

$$x = \frac{\lambda_2}{\beta(\lambda_2 - \lambda_1)} * [e^{\lambda_1 t}(\beta x_0 - \lambda_1 v_0) + f_1(1 - e^{\lambda_1 t})] + \frac{\lambda_1}{\beta(\lambda_2 - \lambda_1)} * [e^{\lambda_2 t}(\lambda_2 v_0 - \beta x_0) - f_1(1 - e^{\lambda_2 t})] \tag{51}$$

$$\dot{x} = \frac{\lambda_1 \lambda_2}{\beta(\lambda_2 - \lambda_1)} * [e^{\lambda_1 t}(\beta x_0 - \lambda_1 v_0) + e^{\lambda_2 t}(\lambda_2 v_0 - \beta x_0) - f_1 e^{\lambda_1 t} + f_1 e^{\lambda_2 t}] \tag{52}$$

$$\ddot{x} = \frac{\lambda_1 \lambda_2}{\beta(\lambda_2 - \lambda_1)} * [\lambda_1 e^{\lambda_1 t}(\beta x_0 - \lambda_1 v_0) + \lambda_2 e^{\lambda_2 t}(\lambda_2 v_0 - \beta x_0) - \lambda_1 f_1 e^{\lambda_1 t} + \lambda_2 f_1 e^{\lambda_2 t}] \tag{53}$$

where $\lambda_1 = \dfrac{-\psi + \sqrt{\psi^2 - 4\beta}}{2}$, and

$$\lambda_2 = \frac{-\psi - \sqrt{\psi^2 - 4\beta}}{2} \tag{54}$$

For the case of $(\psi^2 - 4\beta) < 0$, the general solution can be obtained as follows:

$$x = e^{-\xi\omega t}\left[\left(\frac{v_0 \xi\omega x_0}{\omega_d} - \frac{\xi f_1}{\omega\omega_d}\right)\sin\omega_d t + \left(x_0 - \frac{f_1}{\omega^2}\right)\cos\omega_d t\right] + \frac{f_1}{\omega^2} \tag{55}$$

$$x = \left[-\omega_d\left(x_0 - \frac{f_1}{\omega^2}\right) - \xi\omega\left(\frac{v_o + \xi\omega x_0}{\omega_d} - \frac{\xi f_1}{\omega\omega_d}\right)\right]e^{-\xi\omega t}\sin\omega_d t - \left[\left(x_0 - \frac{f_1}{\omega^2}\right)\xi\omega - \left(v_0 + \xi\omega x_0 - \frac{\xi f_1}{\omega}\right)\right]e^{-\xi\omega t}\cos\omega_d t \tag{56}$$

$$\ddot{x} = \left[\omega_d\left(v_0 + \xi\omega x_0 - \frac{\xi f_1}{\omega}\right) + 2\xi\omega\omega_d\left(x_0 - \frac{f_1}{\omega^2}\right) + (\xi\omega)^2\left(\frac{v_0 + \xi\omega x_0}{\omega_d} - \frac{\xi f_1}{\omega\omega_d}\right)\right]e^{-\xi\omega t}\sin\omega_d t + \left[(\xi\omega)^2\left(x_0 - \frac{f_1}{\omega^2}\right) - \omega_d^2\left(x_0 - \frac{f_1}{\omega^2}\right) - 2\xi\omega\left(v_0 + \xi\omega x_0 - \frac{\xi f_1}{\omega}\right)\right]e^{-\xi\omega t}\cos\omega_d t \tag{57}$$

where $\xi = \dfrac{c}{c_{c1}}$, $c_c = 2m\omega$, $\omega_d = \sqrt{1 - \xi^2}$ (58)

.3.2.2. Secondary impact

The general solution of the occupant response is the same as Equation (43) with a different value of $f(t)$. The value of $f(t)$ is calculated form Equation (40) using the dynamic responses of the fixed structure.

4. NUMERICAL SIMULATIONS

In this section, the analysis developed in the former section is verified by the presentation of the results for both mathematical models. The injury criteria are used to interpret the results. The main injury criterion of interest in this paper is the intrusion criterion, which denotes the interior deformation of the vehicle structure and its effects on the passenger compartment. High impact speeds may result in more severe injuries to vehicle occupants. The intrusion levels depend on how the vehicle structure is assembled and how the impact energy is absorbed by the vehicle structure. The second injury criterion that has been considered is the acceleration level (deceleration) of the occupant. The following two criteria will be used for interpreting the results of the simulation:

(1) Intrusion injury criterion measured as the maximum deformation of the front-end structure.
(2) Deceleration injury criterion measured as the maximum deceleration pulse sustained by occupant during the crash.

A flow chart to demonstrate the process of the solution is shown in Figure 8. The following data are used in the numerical solution. The mass of each vehicle is $m = 1500$ kg (Jawad *et al.*, 1999). The force-deformation characteristic for front - end structure is taken based on the author's previous finite element work and is shown in Figure 5 with the following values: $k_1 = 500$ kN/m, $k_2 = 900$ kN/m with $\delta_c = 0.3$ m. The damping coefficient c_1 is assumed and optimized to be 20 kN·s/m till $v_{dc} = 10$ m/s, and $c_2 = 25$ kN·s/m. The mass of the occupant is $m_o = 65.7$ kg. The occupant's restrained characteristics of the seat

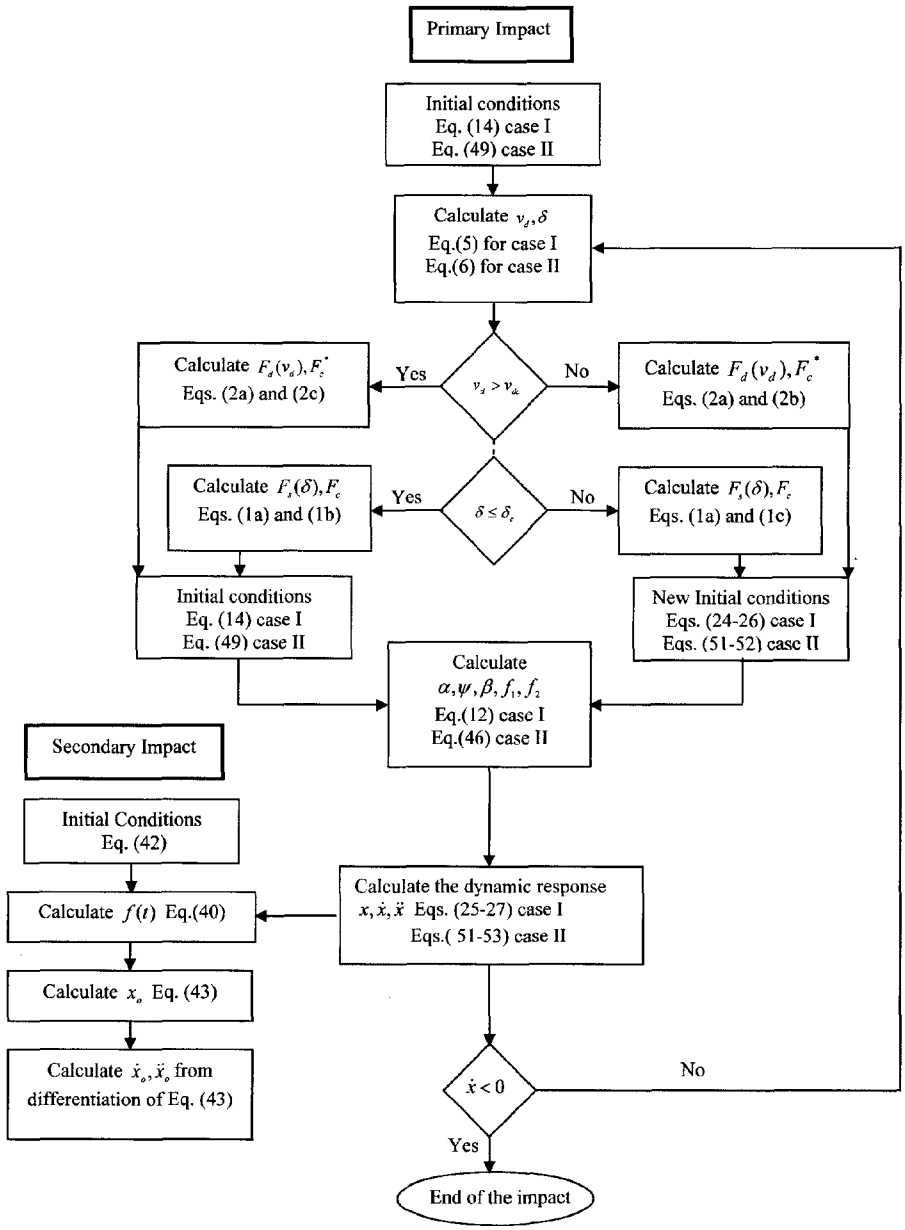

Figure 8. Basic procedure flow chart.

belt and the airbag are represented by stiffness k_o = 98.1 kN/m with slack distance δ_{co} = 0.01 m and damping coefficient c_o = 2.54 kN.s/m (Cacciaube, 1972). The initial velocity of the vehicle and the occupant is v_o = 13.33 m/s. Furthermore, the initial displacement x(0) = x_1 = 0.

4.1. Exendable Smart Structure

The fundamental advantage of smart structures is to absorb more energy for the same crush distance and for the same maximum load level. This is achieved by the ability of smart structures to use more distance available for crush which otherwise is occupied by the folded material of passive structures. The aim of this investigation is to demonstrate the performance of the extendable smart structure in full barrier frontal impact.

Two sets of simulation runs involving a vehicle and a barrier in head-on collision are used. The first set (smart impact) involves a collision of the extendable smart vehicle with the rigid barrier. The hydraulic cylinder is extended by 0.4 m. The second set (standard impact) involves a collision of the standard vehicle with the rigid barrier.

The time history of the total deformation and the acceleration of the occupant, as obtained from the two simulations, are shown in Figures 9 and 10, respectively.

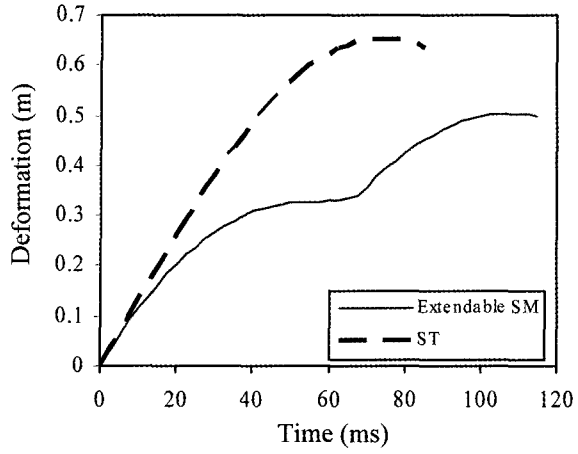

Figure 9. Deformation of the front-end structure (extendable structure).

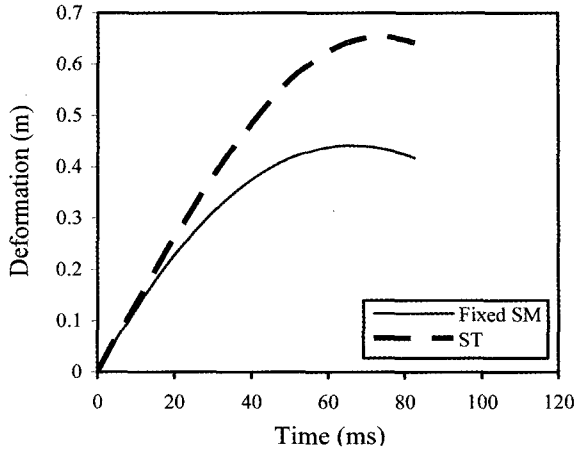

Figure 11. Deformation of the front-end structure (fixed structure).

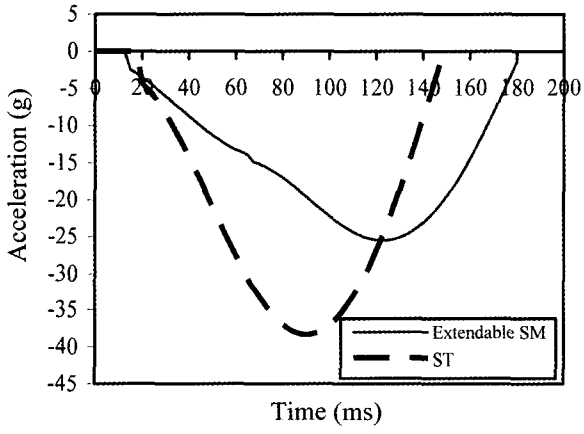

Figure 10. Occupant's acceleration (extendable structure).

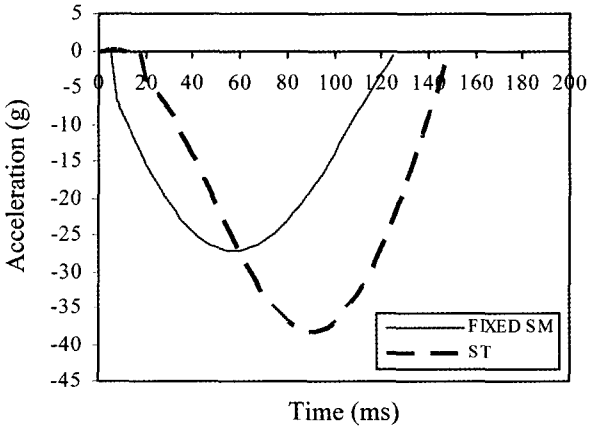

Figure 12. Occupant's acceleration (fixed structure).

The reduction of the deformation is clearly shown in Figure 9. The front-end structure of the standard vehicle is deformed by 0.66 m compared to 0.50 m of the smart vehicle. Furthermore, Figure 10 shows that the peak amplitude of the deceleration of the standard vehicle's occupant appears to be about (38 g) while the corresponding value of the smart vehicle's occupant is considerably smaller (25 g).

4.2. Fixed Smart Structure

The aim of this investigation is to demonstrate the performance of the fixed smart structure in full frontal barrier impact. Two sets of simulation runs involving a vehicle and a barrier in head-on collision are used. The first set (smart impact) involves a collision of the fixed smart vehicle with the rigid barrier. The second set (standard impact) involves a collision of the standard vehicle with the rigid barrier.

Figures 11 and 12 compare the deformation of the front-end structure and the deceleration of the occupant of the two set-ups, respectively. Figure 11 clearly shows the significant reduction in the intrusion injury. This can be concluded by noting that the standard vehicle produced 0.66 m deformation of the front-end structure while in the smart impact, the front-end structure is deformed by 0.44 m. It is clear from Figure 12 that the standard vehicle's occupant suffers higher deceleration (38 g) while the occupant sustains less deceleration (27 g) in the smart impact.

In summary, the significant improvements of both intrusion and deceleration injuries are demonstrated in smart structures in the two cases of simulations. It is clear that the deformations of the front-end structure of the smart structures have magnificent reductions. Furthermore, the deceleration of the occupant is considerably smaller during the time of impact.

5. CONCLUSION

The improved frontal crashworthiness of cars requires totally new design concepts. Two types of smart structures are proposed to support the function of the existing vehicle structure. In addition, two mathematical models representing vehicle-to-barrier impacts for both types of smart structures are introduced and closed form solutions are obtained. It is shown that the mathematical models are valid, flexible, and can be useful in optimization studies. It is proven from numerical simulations that the proposed structures concepts surpass the traditional structures concepts in absorbing crash energy for the same crash distance. Furthermore, it is shown that the smart structure brings significantly lower intrusions and helps keep occupant deceleration within desired limits.

REFERENCES

Appel, H. and Tomasd, J. (1973). The enrgy management structure for the Volkswagen ESV. *SAE Paper No.* 730078.

Cacciaube, A. (1972). Frontal Crash-Influence of the Deceleration Mode (at the Seat Belts Anchorage Points) on Severity Indices. *3rd ESV Conference*, Washington, USA, 141–145.

Clark, C. (1994). The crash anticipating extended airbag bumper system. *14th ESV Conference,* Munich, Germany, 1468–1480.

Coo, P., Janssen, E., Goudswaard, A., Wismans, J. and Rashidy, M. (1991). Simulation model for vehicle performance improvement in lateral collision. *13thESV Conference,* Paris, France, *Paper No.* 91-S5-O-25.

Ellis, E. (1976). Extensible vehicle bumper. *US Patent Office, Pat No.* 3947061.

Jawad, S., Mahmood, H. and Baccouch, M. (1999). Smart structure for improving crashworthiness in vehicle frontal collisions. *The ASME Mechanical Engineering Congress and Exposition*, Nashville, Tennessee, USA, 135–144.

Jawad, S. and Baccouch, M. (2001). Frontal offset crash-smart structure solution. *The ASME Mechanical Engineering Congress and Exposition*, New York, NY, USA, 213–222.

Kamal, M. (1970). Analysis and simulation of vehicle-to-barrier impact. *SAE Trans.* **79**, *SAE Paper No.* 700414.

Reuber, G. and Braun, A. (1994). Bumper system having an extendable bumper for automotive Vehicles. *US Patent Office, Pat No.* 5370429.

Rupp, W. (1974). Front energy management parametric variation study. *5th ESV Conference*, London, England, 602–614.

Schwarz, R. (1971). Hydraulic energy absorption systems for high-energy collisions. *2nd ESV Conference*, Sindelfingen, Germany, Sec. **3**, 36–74.

Wang, J. (1994). Bumper energy absorber. *US Patent Office, Pat No.* 5967573.

Witteman, W. and Kriens, R. (1998). Modeling of an innovative frontal car structure: similar deceleration curves at full overlap, 40 percent offset and 30 degrees collisions. *16th ESV Conference*, Windsor, Ontario, Canada, 194–212.

Witteman, W. (1999). *Improved vehicle crashworthiness design by control of the energy absorption for different collision situations. Ph.D. Dissertation*, Eindhoven University of Technology, Automotive Engineering & Product Design Technology, Eindhoven, The Netherlands.

Witteman, W. and Kriens, R. (2001). The necessity of an adaptive vehicle structure to optimize deceleration pulses for different ceash velocities. *17th ESV Conference*, Amsterdam, The Netherlands, 1–10.